

Direct spectral evidence of single-axis rotation and ortho-hydrogen-assisted nuclear spin conversion of CH₃F in solid para-hydrogen

Yuan-Pern Lee, Yu-Jong Wu, and Jon T. Hougen

Citation: *The Journal of Chemical Physics* **129**, 104502 (2008); doi: 10.1063/1.2975340

View online: <http://dx.doi.org/10.1063/1.2975340>

View Table of Contents: <http://scitation.aip.org/content/aip/journal/jcp/129/10?ver=pdfcov>

Published by the [AIP Publishing](#)

Articles you may be interested in

[Millimeter-wave spectroscopy of H₂C¹³D: Tunneling splitting and ortho-para mixing interaction](#)

J. Chem. Phys. **133**, 154303 (2010); 10.1063/1.3478696

[The hydrogen abstraction reaction H + CH₄. II. Theoretical investigation of the kinetics and dynamics](#)

J. Chem. Phys. **130**, 184315 (2009); 10.1063/1.3132594

[Microcanonical statistical study of ortho-para conversion in the reaction H₃ + H₂ \(H₅\)⁺ → H₃ + H₂ at very low energies](#)

J. Chem. Phys. **126**, 044305 (2007); 10.1063/1.2430711

[Infrared spectra of seeded hydrogen clusters: \(para-H₂\)_N - N₂O and \(ortho-H₂\)_N - N₂O, N = 2 - 13](#)

J. Chem. Phys. **123**, 114314 (2005); 10.1063/1.2032989

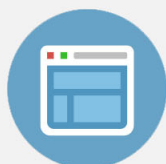
[Selective hyperfine excitation of N₂H⁺ by He: Potential energy surface, cross sections, and propensity rules](#)

J. Chem. Phys. **121**, 4540 (2004); 10.1063/1.1774978



Re-register for Table of Content Alerts

Create a profile.



Sign up today!



Direct spectral evidence of single-axis rotation and *ortho*-hydrogen-assisted nuclear spin conversion of CH₃F in solid *para*-hydrogen

Yuan-Pern Lee,^{1,2,a)} Yu-Jong Wu,^{1,b)} and Jon T. Hougen³¹*Department of Applied Chemistry and Institute of Molecular Science, National Chiao Tung University, 1001, Ta-Hsueh Road, Hsinchu 30010, Taiwan*²*Institute of Atomic and Molecular Sciences, Academia Sinica, Taipei 10617, Taiwan*³*Optical Technology Division, National Institute of Standards and Technology, Gaithersburg, Maryland 20899-8441, USA*

(Received 7 July 2008; accepted 1 August 2008; published online 8 September 2008)

Observation of two weak absorption lines from the E ($K=1$) level and one intense feature from A ($K=0$) for degenerate modes ν_4 and ν_6 of CH₃F provides direct spectral evidence that CH₃F isolated in p -H₂ rotates about only its symmetry axis, and not about the other two axes. An interaction between A and E vibrational levels caused by the partially hindered spinning rotation is proposed. Conversion of nuclear spin between A and E components of CH₃F is rapid when p -H₂ contains some o -H₂, but becomes slow when the proportion of o -H₂ is much decreased. © 2008 American Institute of Physics. [DOI: 10.1063/1.2975340]

I. INTRODUCTION

In conventional matrix-isolation spectroscopy, one employs noble gases such as neon or argon as matrix hosts. Most polyatomic species cannot rotate in these matrices because the solid host is rigid. Only a limited number of small molecules, in particular hydrides, can rotate in noble-gas matrices.¹ *Para*-hydrogen (p -H₂) has emerged as a matrix host^{2,3} because of unique properties associated with the extensive delocalization of the H₂ moieties in this quantum solid, arising ultimately from the fact that the amplitude of the zero-point lattice vibrations is an appreciable fraction of the lattice constant.⁴ Because of the “softness” associated with the quantum solid p -H₂ matrix, the infrared (IR) absorption lines of guest molecules can be extremely narrow, with full widths at half maximum less than 0.01 cm⁻¹.^{5,6}

In addition, guest molecules are expected to rotate in solid p -H₂ more readily than in other matrices.^{7,8} For larger species, molecular rotation is less likely to occur even in solid p -H₂, but internal rotation (torsion) of methyl groups could well persist, as was demonstrated for methanol (which undergoes internal rotation about the C–O bond) by our observation⁹ of splittings of the E/A torsional doublets in internal-rotation-coupled vibrational modes that are qualitatively consistent with those of gaseous CH₃OH. That low-temperature high-resolution spectrum⁹ further revealed a slow conversion of nuclear spin symmetry from species E to A in the host matrix, offering potential insight into nuclear spin conversion in astrophysical sources.¹⁰

The observed torsional doublets of CH₃OH might result in principle from rotational motion of the methyl group against a stationary (in the p -H₂ matrix) hydroxyl group, from rotational motion of the hydroxyl group against a sta-

tionary (in the p -H₂ matrix) methyl group, or from simultaneous rotational motion of both groups against each other (as occurs in the gas phase). To investigate whether the methyl group indeed rotates in p -H₂, we have recorded IR absorption spectra of CH₃F in p -H₂. As explained in more detail below, we observed spectral patterns in the degenerate ν_4 – ν_6 modes indicative of rotation of CH₃F about only its symmetry axis.

II. EXPERIMENTS

In our experiments, a nickel-plated copper block (thickness of 4 mm) served as both a cold substrate for the matrix sample and a mirror to reflect the incident IR beam to the detector.⁹ With a closed-cycle refrigerator system (Janis RDK-415) capable of cooling the sample target to 3.3 K, we can employ conventional continuous deposition with a flow rate ~ 0.03 mol h⁻¹. Typically, a gaseous mixture of CH₃F/ p -H₂ (20–100 ppm, 0.12 mol) or CH₃F/Ar (100 ppm) was deposited over a period of 1–2 h. IR absorption spectra were recorded with a Fourier-transform IR spectrometer (Bomem, DA8) equipped with a KBr beamsplitter and a Hg–Cd–Te detector (cooled to 77 K) to cover the spectral range 500–5000 cm⁻¹. 200 scans at a resolution of 0.05–0.20 cm⁻¹ were generally recorded at each stage of the experiment. CH₃F (98%, PCR Inc.) was purified with a freeze-pump-thaw procedure at 77 K and used with a trap at 253 K to remove trace impurities. H₂ (99.9999%, Scott Specialty Gases) was used after passage through a trap at 77 K before conversion to p -H₂. The p -H₂ converter comprised a copper cell filled with Fe(OH)₃ catalyst and cooled with a closed-cycle refrigerator. The efficiency of conversion is controlled by the temperature of the catalyst; at 15 K, the concentration of o -H₂ is ~ 100 ppm.

^{a)}Author to whom correspondence should be addressed. Electronic mail: yplee@mail.nctu.edu.tw.

^{b)}Present address: National Synchrotron Radiation Research Center, Hsinchu 30076, Taiwan.

III. RESULTS AND DISCUSSION

For interpretation of the observed spectra, we briefly recall some necessary theory. CH_3F is a symmetric-top rotor with C_{3v} symmetry. Its vibrational modes are of either A_1 symmetry (ν_1 to ν_3) or E symmetry (ν_4 to ν_6). According to selection rules, IR absorption bands associated with modes ν_1 – ν_3 of CH_3F are parallel, whereas those associated with the doubly degenerate modes ν_4 – ν_6 are perpendicular. For a symmetric rotor molecule surrounded by atoms or H_2 in a matrix host, it is convenient to distinguish two types of rotation, i.e., a spinning rotation of the molecule about its symmetry axis and a tumbling rotation of the molecule about an axis perpendicular to the symmetry axis. The crystal field is expected to inhibit tumbling rotation far more than spinning rotation in CH_3F . If tumbling is completely quenched, then the two degrees of freedom associated with it turn into librational modes, which behave like (and can therefore be grouped with) the $3N-6=9$ small-amplitude vibrational degrees of freedom in the molecule. If the spinning rotation is nearly unhindered, then the degree of freedom associated with it is expected to quantize like a particle on a ring, giving rise to energy levels of the form AK^2 , where A is the rotational constant of CH_3F about its symmetry axis. From the point of view of quantum numbers, the J and M_J rotational quantum numbers appropriate for an isolated gas-phase molecule in free space are converted, when the symmetric rotor is in the situation described above, into two (near-harmonic-oscillator) librational quantum numbers, while the significance of the K rotational quantum number is largely unchanged. For pictorial visualization, we can consider the CH_3F symmetry axis to be locked in the vertical direction, and the spinning rotational energy levels at AK^2 to correspond to the free-molecule $J=K$ rotational energy levels (which lie at energies of AK^2+BK , where $B \ll A$ is the tumbling rotational constant of CH_3F , and which, in the classical limit, derive all their angular momentum from the spinning motion), so that for CH_3F in $p\text{-H}_2$ only one level ($J=K$) is present in each K stack of a traditional energy level diagram, as shown by the solid lines in Fig. 1.

Vibration-rotation group theory sufficient for the discussion at hand can be described as follows. Consider first the vibrational and rotational coordinate transformations appropriate for the C_{3v} point group.¹¹ Then discard the three σ_v operations since they take a vibrationally distorted and instantaneously chiral molecule from its right-handed to its left-handed form, and are thus not involved in nuclear statistical weight determinations. Discarding these operations also allows us to avoid a discussion here of the precise symmetry of the solid $p\text{-H}_2$ cage containing the CH_3F molecule, i.e., allows us to avoid considering the question of whether or not a change in chirality of the vibrationally distorted molecule can be an isoenergetic feasible operation in that cage. Discarding the three σ_v s is obviously equivalent to keeping only the pure permutations for CH_3F , i.e., to keeping only the identity E , and the permutations (123) and (132), where 1, 2, and 3 are the numerical labels of the three methyl hydrogens. The (123) operation is clearly isoenergetic, since it corresponds physically to a $2\pi/3$ change in the spinning angle,

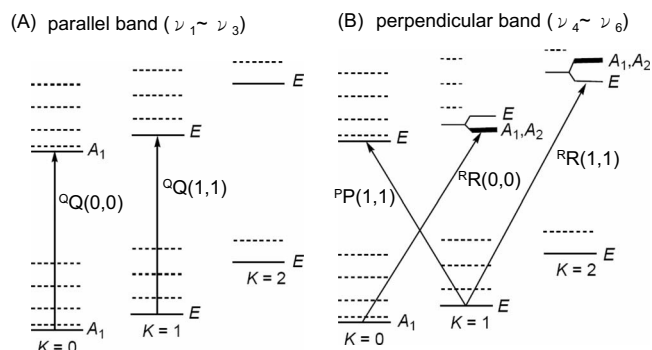


FIG. 1. Energy levels and transitions of CH_3F in $p\text{-H}_2$. If only spinning rotation occurs, all $J>K$ levels in each K stack (shown as dashed lines) are shifted to much higher (librational) energies, leaving only the $J=K$ level in each stack (solid line) at approximately its gas-phase energy. Only these $J=K$ levels of the ground vibrational state are then populated at low temperatures, so that a single line is expected for the ν_1 – ν_3 fundamental bands, whereas three lines are expected for ν_4 – ν_6 , as indicated by the arrows in this figure. (Note that the A_1, A_2-E Coriolis splittings in the upper vibrational state in (b), which correspond to parallel or antiparallel orientations of the spinning rotational angular momentum with respect to the vibrational angular momentum in the E vibrational state, are shown for a positive value of the Coriolis coupling constant ζ .)

together with changes in the vibrational displacements such that the final molecular orientation and shape in the cage is just as it was, except for a relabeling of identical hydrogen nuclei.¹¹ The (123) operation is also feasible under our assumption of a nearly unhindered spinning rotation. Without going into detail, the rotational subgroup C_3 containing the three operations E , $C_3=(123)$, and $C_3^2=(123)^2$ is all that is required to determine nuclear spin statistics, and this group preserves the nuclear spin statistics of the free molecule, since spinning levels with $K=0$ modulo 3 belong to the non-degenerate symmetry species A (with total hydrogen nuclear spin $I=3/2$), while spinning levels with $K \neq 0$ modulo 3 belong to the doubly degenerate symmetry species E (with total hydrogen nuclear spin $I=1/2$).

At very low temperatures, we should thus have only $K=0$ molecules with $I=3/2$ nuclear spin functions and $K=1$ molecules with $I=1/2$ nuclear spin functions. Furthermore, we expect the angular momentum of the spinning $K=\pm 1$ molecules to be aligned parallel or antiparallel to the vibrational angular momentum $\ell=\pm 1$ of the degenerate vibrational fundamentals to give rise to first-order Coriolis splitting analogous to those caused by the term $-2AK\zeta\ell$ in the gas phase, and illustrated schematically in Fig. 1(b). Thus, if CH_3F undergoes only spinning rotation in solid $p\text{-H}_2$ at low temperatures, we expect to observe in the IR spectrum of its three parallel bands ν_1 – ν_3 a single line containing the superimposed (i.e., unresolved) $K=0 \leftarrow 0$ A line and $K=1 \leftarrow 1$ E line. On the other hand, for the three perpendicular bands ν_4 – ν_6 , one expects to observe three lines, consisting of an intense central line, denoted ${}^{\text{R}}\text{R}(0,0)$ in gas-phase $\Delta^K \Delta J(J,K)$ notation, and two weak features, ${}^{\text{P}}\text{P}(1,1)$ and ${}^{\text{R}}\text{R}(1,1)$, one on either side of the ${}^{\text{R}}\text{R}(0,0)$ line, as indicated by the arrows in Fig. 1.

Previous investigations of the rotation of CH_3F in matrices have focused on only the band shape of the most intense single line near 1040 cm^{-1} associated with the CF stretching

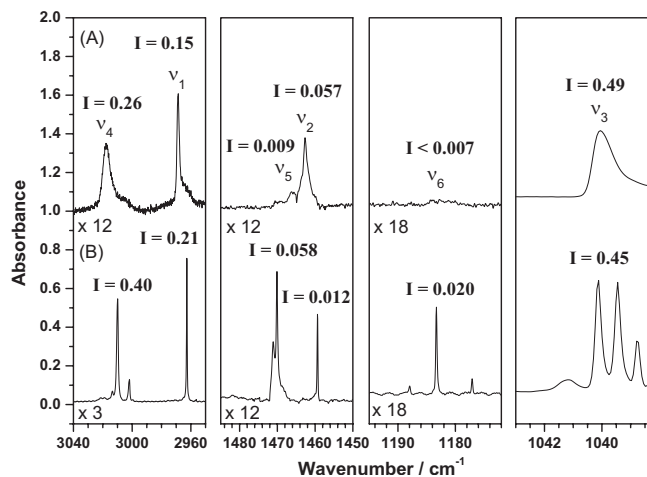


FIG. 2. Survey IR absorption spectra of matrix-isolated CH₃F. (a) CH₃F/Ar (1/10 000); (b) CH₃F/*p*-H₂ (1/15 000). For each acquisition of spectral data, 200 scans at a resolution 0.1 cm⁻¹ were accumulated during ~0.5 h. The sample was at 3.3 K. Integrated band intensities *I* are shown above each band.

(ν_3) mode. Because many factors affect the band shape, information from these experiments on whether CH₃F rotates^{12,13} or not^{14,15} in solid Ar is inconclusive.

Overview spectra of CH₃F/Ar (~100 ppm, 0.05 mol) and CH₃F/*p*-H₂ (~70 ppm, 0.04 mol) at 3.3 K after deposition are shown in Fig. 2. The implications of these spectra are most easily understood if each wavenumber region is considered separately.

The C–F stretching (ν_3) mode near 1040 cm⁻¹ shows multiple lines in *p*-H₂, which were assigned previously by Yoshioka and Anderson¹⁶ to CH₃F complexed with various numbers of *o*-H₂ due to their large polarity. Typically in their experiments *o*-H₂ was initially present as an impurity to an extent of ~100 ppm or more, but after several hours the concentration of *o*-H₂ decreases, and eventually only the isolated CH₃F dominates, giving rise to a single peak, in agreement with expectations for a parallel band, as illustrated in Fig. 1(a). The integrated intensities *I* obtained from our

spectra are given above each band in Fig. 2. It can be seen that these intensity values are nearly equal for the ν_3 mode in our Ar and *p*-H₂ spectra.

The degenerate C–F rocking (ν_6) mode near 1180 cm⁻¹ is barely visible in solid Ar, but shows a clear triplet pattern in *p*-H₂, which is consistent with expectations for a perpendicular band when only rotation about the symmetry axis occurs, as illustrated in Fig. 1(b). Ignoring centrifugal distortion effects, the three lines in this triplet should occur at the following approximate frequencies:

$${}^R R(1,1) = \nu_0 + 4A' - 4A'\zeta' - A'',$$

$${}^R R(0,0) = \nu_0 + A' - 2A'\zeta',$$

$${}^P P(1,1) = \nu_0 - A''. \quad (1)$$

These three equations and the measured line positions in Table I can be used to obtain

$$\nu_0 - A' = 1177.85 \text{ cm}^{-1} (\approx 1177.47 \text{ cm}^{-1}),$$

$$A' - A'' = -0.75 \text{ cm}^{-1} (\neq +0.024 \text{ cm}^{-1}),$$

$$A'(1 - \zeta') = +2.725 \text{ cm}^{-1} (\approx +3.662 \text{ cm}^{-1}), \quad (2)$$

for ν_6 . The values in parentheses are calculated from the gas-phase spectroscopic constants^{17,18} of CH₃F.

It is well known that the rotational constants of molecules in helium droplets and *p*-H₂ are decreased somewhat from their gas-phase values because of the drag of the solvent molecules. One possibility for explaining the large negative value for $A' - A''$ in *p*-H₂, compared to the much smaller positive value in the gas phase, is thus to suppose that the vibrating molecule in the $\nu_6=1$ state experiences more drag in *p*-H₂ than does the ground state molecule. This postulated decrease in A' can then also be used to explain the smaller value of $A'(1 - \zeta')$ in *p*-H₂ compared to the gas phase. Assuming that the vibrational parameter ζ' is largely unchanged in the matrix (like the vibrational frequency), we

TABLE I. Comparison of line positions [uncertainties (type B, $k=1$) are 1 in the last digit given for the gas-phase and solid *p*-H₂ measurements, and 3 in the last digit given for the solid Ar measurements (Ref. 22)] of CH₃F isolated in solid Ar, solid *p*-H₂, and in the gaseous phase.

Mode	Description	Sym.	$\Delta^K \Delta J(J, K)$	Gas ^a (cm ⁻¹)	Solid Ar ^b (cm ⁻¹)	Solid <i>p</i> -H ₂ (cm ⁻¹)
ν_1	CH sym. stretch	A ₁	${}^Q Q(0,0)$	2966.25	2968.6	2962.7
ν_2	CH sym. deformation	A ₁	${}^Q Q(0,0)$	1459.39	1462.6	1470.1?
ν_3	CF stretch	A ₁	${}^Q Q(0,0)$	1048.61	1040.1	1040.2
ν_4	CH asym. stretch	E	${}^R R(0,0)$	3010.76	3017.9	3009.8
			${}^P P(1,1)$	2999.78		3001.9
			${}^R R(1,1)$	3020.03		3013.4
ν_5	CH asym. deformation	E	${}^R R(0,0)$	1476.39	1466.7	1470.1
			${}^P P(1,1)$	1461.78		1459.3
			${}^R R(1,1)$	1489.19		1471.1?
ν_6	CH ₃ rock	E	${}^R R(0,0)$	1185.64	1182.1	1183.3
			${}^P P(1,1)$	1176.64		1177.1
			${}^R R(1,1)$	1192.96		1188.0

^a ν_1 and ν_4 from Refs. 20 and 21, ν_2 , ν_3 , and ν_5 from Ref. 18, and ν_6 from Refs. 17 and 18.

^bReference 14 and this work.

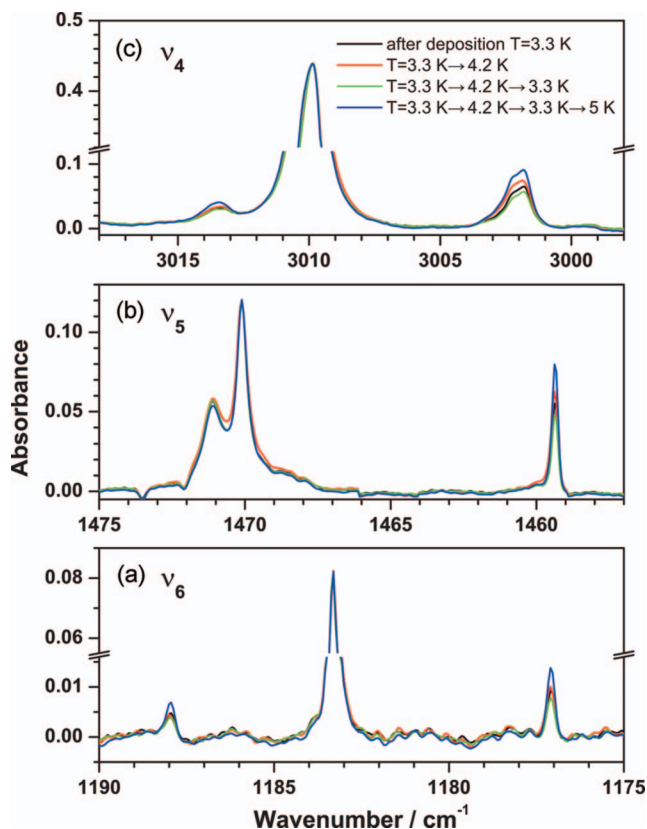


FIG. 3. (Color) Partial IR absorption spectra of (a) ν_6 , (b) ν_5 , and (c) ν_4 modes of a $\text{CH}_3\text{F}/p\text{-H}_2$ (1/15 000) matrix sample after deposition at 3.3 K (black), raising the temperature to 4.2 K (red), decreasing the temperature to 3.3 K (green), and again raising the temperature to 5.0 K (blue). All spectra were normalized to the ${}^R R(0,0)$ line.

calculate that A' decreases from 5.21 cm^{-1} in the gas phase to 3.87 cm^{-1} in the matrix, which then leads to a smaller decrease of A'' from 5.18 to 4.62 cm^{-1} in the matrix.

For the triplet explanation given above to be correct, the two weak outer features must be “hot-band” transitions from the $K=1$ level. To test this, we performed temperature cycling experiments by raising the temperature of the matrix to 4.2 K, followed by cooling to 3.3 K, then warming to 5.0 K. Spectra of ν_6 recorded at each stage and normalized to the intense central ${}^R R(0,0)$ feature are shown in Fig. 3(a). The intensity of the central feature will also vary with temperature because of lower state population changes, but we nevertheless chose to normalize our various scans to this peak in order to remove the effects of sample evaporation during the temperature cycling procedure. The variation of intensity of the weak features at 1177.1 and 1188.0 cm^{-1} relative to the intense feature at 1183.3 cm^{-1} depends on temperature, and cycles reproducibly. Assuming a Boltzmann distribution for $K=0$ and 1 levels of the vibrational ground state, we deduce from the observed relative intensity an energy gap $\sim 5.5 \pm 1.5 \text{ cm}^{-1}$, in reasonable agreement with the gap of $\sim 4.6 \text{ cm}^{-1}$ (6.0 cm^{-1} in the gas phase) expected from our model of spinning rotational energy levels given by AK^2 for CH_3F in $p\text{-H}_2$.

From our integrated intensities, it appears that the intensity of ν_6 is significantly greater in $p\text{-H}_2$ than in Ar. Furthermore, it is known that the ν_6 perpendicular band gains inten-

sity in the gas phase from the much stronger ν_3 parallel band via a Coriolis mixing induced by the tumbling rotation.¹⁹ If, as the present experiments strongly suggest, tumbling rotations are quenched in $p\text{-H}_2$, then such a Coriolis interaction becomes impossible. In its place, however, a rather different mechanism arises for mixing A_1 and E vibrational states in $p\text{-H}_2$, involving the (slightly hindered) spinning rotation. We can use the C_3 group theory described earlier to note that a vibration-rotation interaction term of the form $\cos(\chi + \varphi_v)$ is totally symmetric,¹¹ where χ is the angle associated with the spinning rotation and φ_v is the angle associated with a degenerate E vibration expressed in polar coordinates. This term is absent for a gas-phase molecule because the potential energy in free space cannot depend on the rotational angles. This term will have almost no effect in a solid Ar matrix if one assumes that the spinning rotation is quenched, i.e., if one assumes that χ is frozen at some fixed value. On the other hand, in solid $p\text{-H}_2$, we have concluded on the basis of the ν_6 triplet pattern analysis above that a somewhat hindered spinning rotation occurs. This causes the potential energy to be χ -dependent, and the $\cos(\chi + \varphi_v)$ term chosen above has exactly the correct form to permit the ${}^{\nu} E$ rovibrational level with $K=0$ in a ${}^{\nu} E$ vibrational state [Fig. 1(b)] to mix with (and borrow intensity from) the ${}^{\nu} E$ rovibrational level with $K=1$ in a ${}^{\nu} A$ vibrational state [Fig. 1(a)], or to permit the ${}^{\nu} A$ component of the $K=1$ level of a ${}^{\nu} E$ vibrational state [Fig. 1(b)] to mix with the ${}^{\nu} A$ level with $K=0$ in a ${}^{\nu} A$ vibrational state [Fig. 1(a)], where the left superscripts ν and νr are introduced to distinguish between vibrational and rovibrational (i.e., vibration-spinning-rotation) symmetry species, respectively.

The $\nu_2(A_1)/\nu_5(E)$ band pair near 1470 cm^{-1} is rather complicated. If the integrated intensities are used as a guide, it appears that $\nu_2 < \nu_5$ in solid Ar, while $\nu_2 > \nu_5$ in $p\text{-H}_2$. These two close lying fundamentals are also known to undergo a strong Coriolis interaction in the gas phase induced by the tumbling rotation.¹⁹ For our $p\text{-H}_2$ spectra, we believe it is interactions caused by the $\cos(\chi + \varphi_v)$ term discussed above (perhaps acting in concert with some of its higher-order analogs) that prevents this $\nu_2(A_1)/\nu_5(E)$ region from being a clear superposition of a pure-parallel-band single-line spectrum and a pure-perpendicular-band triplet pattern. This same term can again provide a mechanism for explaining the somewhat larger integrated intensities of the ν_5 perpendicular band in $p\text{-H}_2$ versus Ar, via intensity borrowing from the strong ν_2 parallel band.

The $\nu_1(A_1)/\nu_4(E)$ region near 3000 cm^{-1} does in fact look like the superposition of a single line parallel band pattern and a triplet perpendicular band pattern, except that we must choose between a sharp line and a broad line for the high-wavenumber triplet component. Choosing the sharp line is appealing because its shape resembles the other two lines; choosing the broad line is appealing because the two outer triplet components are then approximately symmetrically displaced from the central component. The temperature cycling studies in Fig. 3(c) indicate that we must choose the sharp component. Making this choice, we can again use Eq. (1) to derive a set of values for the various spectroscopic constants, but the value for A'' derived from the $\nu_1(A_1)/\nu_4(E)$

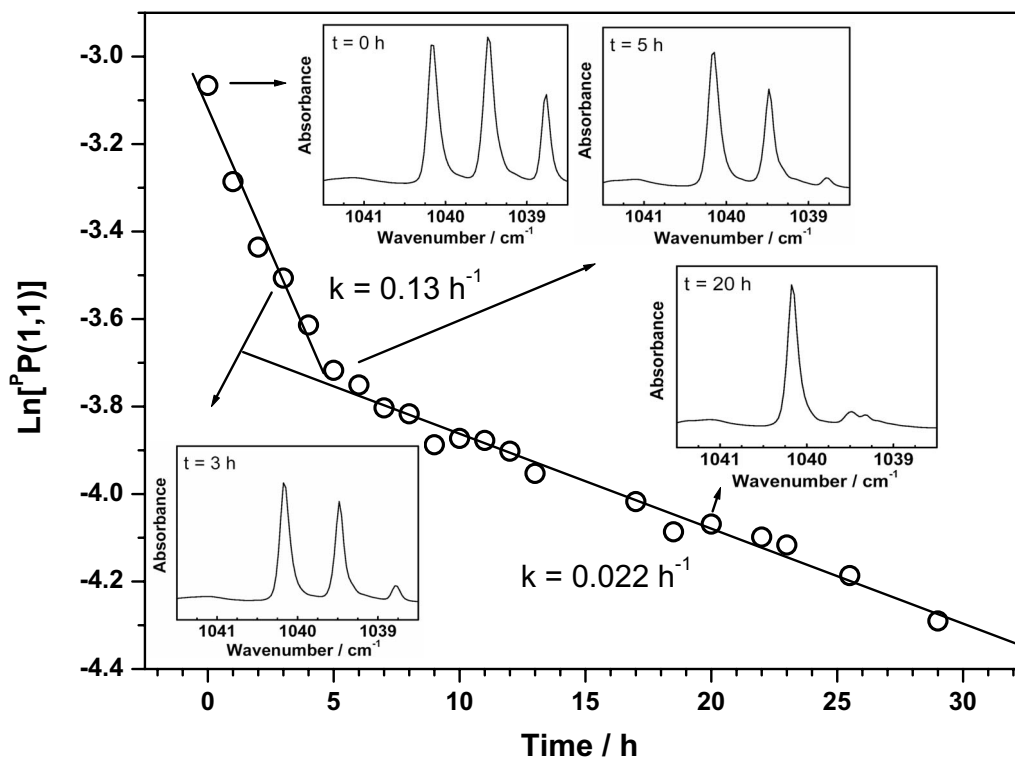


FIG. 4. Decay of the integrated intensity of band $P(1,1)$ as a function of time. The spectra of CH₃F in the ν_3 region at some periods are also illustrated.

pattern is not in good agreement with the value derived from the $\nu_6(A_1)$ pattern. Since the $\nu_1(A_1)/\nu_4(E)$ region in the gas phase is known to be highly perturbed by many other states^{20,21} and since we do not have enough information to take any of these interactions into account here, we have not pursued a quantitative treatment of this region.

It is interesting to note that only ν_3 (the C–F stretch) shows significant additional structure when *o*-H₂ is present (see Fig. 2). As pointed out by the referee, this suggests that the “bonded” *o*-H₂ molecules lie in sites off the end of the F atom. Such positions, which also seem reasonable electrostatically, would maximize the influence of bonded *o*-H₂ molecules on the C–F stretching frequency and minimize their influence on the methyl hydrogen stretching and bending frequencies. Influence on the C–F bend would presumably be intermediate between these two extremes, with the resulting absence of observed extra structure on ν_6 suggesting that the C–F bending frequency is also not significantly perturbed by the axially bonded *o*-H₂ molecules.

The fact that the relative intensities of bands associated with levels $K=0$ and $K=1$ vary with temperature indicates that the time for nuclear-spin conversion (NSC) is smaller than the time required for temperature changes and data acquisition. This interconversion between populations of $K=1$ (*E* symmetry) and $K=0$ (*A* symmetry) in the vibrational ground state of CH₃F can occur only via conversion of the total nuclear spin of CH₃ between $I=3/2$ and $1/2$. We observed, however, that after ~ 5 h temperature cycling experiments yield no observable variation in intensity for the two weak features relative to the intense one, indicative that NSC becomes slow when the concentration of *o*-H₂ impurity molecules in contact with the CH₃F is diminished. It seems rea-

sonable to assume that nearby *o*-H₂ molecules enhance NSC because of various magnetic interactions of the nonzero nuclear spin of *o*-H₂ with the nuclear spins of the methyl hydrogens. Plotting the intensity ratio of lines $P(1,1)$ and $R(0,0)$ of CH₃F at 3.3 K as a function of time, we found a biexponential decay, as shown in Fig. 4. The rate coefficient for the spin conversion from *E* to *A* components of CH₃F decreased from $\sim(0.13 \pm 0.03) \text{ h}^{-1}$ at the initial stage to $\sim(0.022 \pm 0.005) \text{ h}^{-1}$ after 5 h. The ν_3 region, where the multiple-line structure is indicative of the proportion of *o*-H₂ present in the matrix, is shown also as insets to demonstrate the diminishing proportion of *o*-H₂ attached to CH₃F with increasing duration after formation of the solid sample. This correlation provides direct evidence that the presence of *o*-H₂ enhances the rate of NSC. For comparison, the rate coefficient for NSC from *E* to *A* components of CH₃OH at 3.5 K was determined to be $\sim(0.018 \pm 0.003) \text{ h}^{-1}$.⁹

In conclusion, the observation here of a nearly symmetrical triplet line pattern for ν_6 , the most isolated of the three degenerate vibrations in CH₃F, with the two weak outer features in the pattern showing the predicted temperature-dependent intensities, provides the first direct spectral evidence that a molecule such as CH₃F isolated in *p*-H₂ undergoes rotation about its symmetry axis, but not about the other two axes. A new type of interaction between the spinning-rotation and the angular momentum of a degenerate vibration in CH₃F, which arises because the spinning rotation of the molecule is partially hindered in the matrix, is proposed to allow mixing between *A* and *E* vibrational states, and thus to rationalize the complicated absorption patterns observed when an *A* and *E* vibrational level are nearly degenerate in CH₃F. The presence of *o*-H₂ in the matrix enhances nuclear

spin conversion. After the concentration of *o*-H₂ has decayed with time, the measured rate coefficient for the conversion of nuclear spin from *E* to *A* components of CH₃F at 3.3 K is determined to be similar to that observed for CH₃OH in *p*-H₂.

ACKNOWLEDGMENTS

We thank the National Science Council of Taiwan (Grant No. NSC96-2113-M009-025) and the Ministry of Education (MOE-ATU project) for support.

- ¹A. J. Barnes, W. J. Orville-Thomas, A. Müller, and R. Gaufrès, *Matrix Isolation Spectroscopy* (Reidel, Dordrecht, 1981).
- ²T. Oka, *Annu. Rev. Phys. Chem.* **44**, 299 (1993).
- ³T. Momose and T. Shida, *Bull. Chem. Soc. Jpn.* **71**, 1 (1998).
- ⁴J. van Kranendonk, *Solid Hydrogen: Theory of the Properties of Solid H₂, HD, and D₂* (Plenum, New York, 1983).
- ⁵S. Tam, M. E. Fajardo, H. Katsuki, T. Wakabayashi, and T. Momose, *J. Chem. Phys.* **111**, 4191 (1999).
- ⁶T. Momose, M. Miki, T. Wakabayashi, T. Shida, M.-H. Chan, S. S. Lee, and T. Oka, *J. Chem. Phys.* **107**, 7707 (1997).
- ⁷H. Hoshina, T. Wakabayashi, T. Momose, and T. Shida, *J. Chem. Phys.*

- 110**, 5728 (1999).
- ⁸T. Momose, H. Hoshina, M. Fushitani, and H. Katsuki, *Vib. Spectrosc.* **34**, 95 (2004).
- ⁹Y.-P. Lee, Y.-J. Wu, R. M. Lees, L.-H. Xu, and J. T. Hougen, *Science* **311**, 365 (2006).
- ¹⁰M. J. Mumma, H. A. Weaver, and H. P. Larson, *Astron. Astrophys.* **187**, 419 (1987).
- ¹¹J. T. Hougen, *J. Chem. Phys.* **37**, 1433 (1962).
- ¹²V. A. Apkarian and E. Weitz, *J. Chem. Phys.* **76**, 5796 (1982).
- ¹³B. Gauthier-Roy, L. Abouaf-Marguin, and F. Legay, *Chem. Phys.* **46**, 31 (1980).
- ¹⁴L. H. Jones and B. I. Swanson, *J. Chem. Phys.* **76**, 1634 (1982).
- ¹⁵L. H. Jones and B. I. Swanson, *J. Chem. Phys.* **77**, 6338 (1982).
- ¹⁶K. Yoshioka and D. T. Anderson, *J. Chem. Phys.* **119**, 4731 (2003).
- ¹⁷D. Papoušek, R. Tesař, P. Pracna, S. Civiš, M. Winnewisser, S. P. Belov, and M. Y. Tretyakov, *J. Mol. Spectrosc.* **147**, 279 (1991).
- ¹⁸D. Papoušek, P. Pracna, M. Winnewisser, S. Klee, and J. Demaison, *J. Mol. Spectrosc.* **196**, 319 (1999).
- ¹⁹C. di Lauro and I. M. Mills, *J. Mol. Spectrosc.* **21**, 386 (1966).
- ²⁰J. P. Champion, A. G. Robiette, I. M. Mills, and G. Graner, *J. Mol. Spectrosc.* **96**, 422 (1982).
- ²¹G. Graner and G. Guelachvili, *J. Mol. Spectrosc.* **89**, 19 (1981).
- ²²B. N. Taylor and C. E. Kuyatt, NIST Technical Note No. 1297, 1994; this publication may be downloaded from <http://physics.nist.gov/Pubs/guidelines/contents.html>.